New Journal of Physics
The open access journal at the forefront of physics

Deutsche Physikalische Gesellschaft DPG
IOP Institute of Physics

Published in partnership with: Deutsche Physikalische Gesellschaft and the Institute of Physics

OPEN ACCESS

RECEIVED
22 October 2019

REVISED
23 January 2020

ACCEPTED FOR PUBLICATION
10 February 2020

PUBLISHED
19 March 2020

PAPER

Spin decoherence in inhomogeneous media

J A Crosse[1,2]

[1] New York University Shanghai, 1555 Century Avenue, Pudong, Shanghai, 200122, People's Republic of China
[2] NYU-ECNU Institute of Physics at NYU Shanghai, 3663 Zhongshan Road North, Shanghai, 200062, People's Republic of China

E-mail: jac32@nyu.edu

Keywords: spin decoherence, macroscopic quantum electrodynamics, surface-induced relaxation, electromagnetic green's function, local-field corrections

Supplementary material for this article is available online

Abstract

A Green's function formalism for describing the decoherence of a 'central spin' in inhomogeneous media is developed. By embedding the 'central spin' in a background medium and performing real-cavity, local-field corrections on the macroscopic fields at the location of the 'central spin' one can show that the Green's function splits up into two main contributions, a contribution that is related to the bulk properties of the background medium and a contribution that is related inhomogeneities within the background medium. As an example, the coherence time of a shallow *NV* center in diamond close to a planar interface, both in the absence and presence of surface spins, is computed. It is found that the coherence time of the *NV* center increases as it moves away from the interface and, at distances greater than ≈1 nm, the interaction with the interface is negligible with the main source of decoherence coming from the interaction with the surface spins. Above ≈50 nm the interaction with the surface spins is also negligible and one recovers the bulk coherence time.

1. Introduction

Owing to their ability to generate and maintain coherent superpositions, single spin qubits show much promise as a platform for realizing quantum computing and quantum information processing [1, 2]. However, as these spins are unavoidably coupled to the environment, the coherence times of these superposition states is finite and, if left to freely evolve, the spin will 'decohere' to a mixed state of the two eigenstates [3, 4]. This finite coherence time is a major limiting factor in the realization of many quantum information protocols.

For many spin systems the main source of decoherence is the interaction with nuclear spins in the surrounding material. For example, the main source of decoherence for phosphorus donors in silicon are the ^{29}Si isotopes that are present at a concentration of about 4.7% in natural silicon [5] and, likewise, ^{13}C, at a concentration of about 1.1%, are the primary source of decoherence for NV centers in diamond [6]. The main technique for modeling decoherence is to use a microscopic spin-bath model [4] where one couples the 'central spin' individually to a bath nuclear spins. Further interactions couple the nuclear spins within the bath inducing intrabath correlations which also affect the coherence properties of the 'central spin' [7]. The coherence time can then be computed by applying one of the usual cluster-expansion techniques by which one can obtain a numerically tractable expression. Despite this, for large systems, these methods can be computationally intensive. Furthermore, although one can specify the exact position of the bath spins within the spin bath, this technique proves awkward when one needs to consider inhomogeneities in the medium in which the 'central spin' is embedded. An example of this can be seen when one considers a 'central spin' located close to an interface (shallow NV centers, which can be located within several nanometers of the diamond surface, would be an example of such a system). Naively, one may think that as the 'central spin' approaches the surface the coherence time will increase as the number of nearby nuclear spins decreases. However, experimental work has shown that this is not the case and, in fact, the coherence time decreases dramatically close to the surface [8, 9]. A

number of phenomenological models have been constructed to account for this effect [10, 11] but a general framework for studying such systems is absent.

Previously, it was shown that, by considering a spin-boson model and expanding the bosonic modes of the environment using the macroscopic quantum electrodynamics formalism [12, 13], one can obtain an expression for the decoherence of a 'central spin' in terms of the electromagnetic Green's function of the surrounding material [14]. By substituting the homogeneous Green's function into the general expression, the coherence time for a spin in an infinitely extended medium can be found. However, the Green's function formalism applies to any general material geometry and by replacing the homogeneous Green's function with the appropriate inhomogeneous Green's function the coherence time within an inhomogeneous medium can also be computed.

Here, we extend the Green's function formalism of spin decoherence from homogeneous media to inhomogeneous media and compute analytical expressions for the coherence time for a 'central spin' close to a surface and in the presence of surface spins. Although we only consider planar layered geometries here, the Green's function formalism is general and, hence, applicable to any material configuration. Analytical expressions for the coherence time can be obtained for regular geometries (planes, cylinders, spheres, etc) where a closed form expression for the Green's function are known. For non-regular geometries, numerical methods for computing the Green's function for arbitrary media are well developed. For example, similar computation techniques are required to compute Casimir and Casimir–Polder interactions, which have been implemented in the computational package SCUFF-EM [15]. Hence, numerical methods are already available to implement the following theory, which would allow one to calculate spin coherence under any material geometry.

2. Theory

2.1. The spin-boson model

Consider a spin-boson model where a two-level, 'central spin', described by the spin operator, $\hat{\mathbf{S}}$, is placed in a magnetic field, orientated in the z-direction, and coupled to an 'environment' consisting of magnetic fluctuations described by a bath of bosonic operators, $\hat{\mathbf{b}}(\mathbf{r},\ t)$. The dynamics of a 'central spin' subject to a magnetic field are governed by the Zeeman Hamiltonian

$$H_0 = \omega_0 \hat{S}_z, \tag{1}$$

with the two energy levels, corresponding to the 'spin up' and 'spin down' eigenstates, separated by an energy $\Delta E = 2\omega_0$. The interaction with the magnetic fluctuations can be described by an interaction term of the form [4]

$$H_{\mathrm{I}} = \gamma \hat{\mathbf{S}} \cdot \hat{\mathbf{b}}(\mathbf{r},\ t), \tag{2}$$

where we assume the energy of the fluctuations described by the operator $\hat{\mathbf{b}}(\mathbf{r},\ t)$ are much smaller than the energy splitting of the spin eigenstates, ΔE, and hence the interaction with the environment can be treated as a small perturbation. Here, the coupling strength between the 'central spin' and the magnetic fluctuations is given by the gyromagnetic ratio $\gamma = g\mu_B/\hbar$, where g is the landé g-factor and μ_B is the bohr magnaton.

The transverse part of the interaction Hamiltonian induces spin flips which relaxes the higher energy spin state to the lower energy spin state, or equivalently leads to the decay of the certain diagonal elements of the spin's density matrix. This class of Hamiltonian has been extensively studied (notably in [3]) and, from the dynamics of the 'central spin' subject to such an interaction, a characteristic time for this relaxation process, usually designated T_1, can be computed.

The longitudinal part of the interaction Hamiltonian induces pure dephasing which leads to loss of coherence of the two spin states, i.e. the decay of the off-diagonal elements of the spin's density matrix. The characteristic time for this process is usually designated T_2, and is usually less than T_1 ($T_2 < T_1$). Here, we will consider the longitudinal problem as this is the main limiting process for quantum technology. The longitudinal problem also has the advantage that the interaction Hamiltonian commutes with the Zeeman Hamiltonian and hence the eigenstates of the $\hat{S}_z$ are unchanged by the interaction.

To simplify the analysis one can remove the free evolution of the spin by moving to the interaction picture. It also proves to be convenient to write the magnetic fluctuations as a sum of their modes. In this new frame the 'central spin' evolves under the Hamiltonian

$$\hat{H}(t) = \gamma \hat{S}_z \int_0^\infty \mathrm{d}\omega [\hat{b}_z(\mathbf{r}_\mathrm{s},\ \omega,\ t) + \hat{b}_z^\dagger(\mathbf{r}_\mathrm{s},\ \omega,\ t)]. \tag{3}$$

The coherence, $L(t)$, of a 'central spin' can be found by taking the expectation value of the coherence operator $\hat{S}_+ = \hat{S}_x + \mathrm{i}\hat{S}_y$,

$$L(t) = \langle \hat{S}_+ \rangle = L(0)\mathrm{e}^{-\phi(t)}, \tag{4}$$

with the function, $\phi(t)$, giving the decoherence rate as a function of time, t.

2.2. Magnetic fluctuations

We wish to find a bosonic operator that correctly describes the magnetic fluctuations of the environment. In any dissipative system, the act of dissipation results in the generation of noise. This is formally described by the fluctuation-dissipation theorem which relates the power spectrum of the noise to the imaginary part of the response function. An example of this would be Johnson noise in a resistor. The energy dissipated by the resistor when a current flows leads to heating and the resulting thermal fluctuations, in turn, drive noise currents. Thus, noise is generated in the resistor by the dissipation process. Similar processes generate noise in all absorbing media. As absorption is a necessary consequence of the Kramers–Krönig relations, which themselves are a consequence of causality [16], then one would expect absorption, and hence noise, in any responding system.

It is possible to derive a quantum field theory description of such noise by considering a three part coupled system where an external electromagnetic field interacts with a matter field which, in turn, is coupled to a bath of oscillators that models absorption. This system can be quantized from first principles to give a set of bosonic operators that describe collective excitations of the field-matter-bath system (the somewhat lengthy calculation is documented in detail in [17, 18]). When one substitutes the expressions for these bosonic operators into the expressions for the macroscopic electromagnetic fields one finds that the displacement field, $\hat{\mathbf{D}}(\mathbf{r}, \omega)$, gains extra terms that can be shown to have the properties of Langevin noise sources. This noise term originates from the coupling to the oscillator bath and, hence, is a result of the absorptive properties of the system. This absorption driven noise can therefore be identified with the noise predicted by the fluctuation dissipation theorem. Separating these extra terms from the usual expression for the displacement field, $\hat{\mathbf{D}}(\mathbf{r}, \omega)$, leads to two new 'noise' fields which are associated with the electric and magnetic fluctuations respectively. The quantization scheme described above allows one two write these two 'noise' fields in terms of two sets of canonical bosonic operators, $\hat{f}_e(\mathbf{r}, \omega)$ and $\hat{f}_m(\mathbf{r}, \omega)$, as

$$\hat{\mathbf{P}}_N(\mathbf{r}, \omega) = \mathrm{i}\sqrt{\frac{\hbar\varepsilon_0}{\pi}\,\mathrm{Im}\,\varepsilon(\mathbf{r}, \omega)}\;\hat{\mathbf{f}}_e(\mathbf{r}, \omega), \tag{5}$$

$$\hat{\mathbf{M}}_N(\mathbf{r}, \omega) = \sqrt{\frac{\hbar}{\mu_0\pi}\frac{\mathrm{Im}\,\mu(\mathbf{r}, \omega)}{|\mu(\mathbf{r}, \omega)|^2}}\;\hat{\mathbf{f}}_m(\mathbf{r}, \omega). \tag{6}$$

The 'noise' fields $\hat{\mathbf{P}}_N(\mathbf{r}, \omega)$ and $\hat{\mathbf{M}}_N(\mathbf{r}, \omega)$ are termed the noise polarization and noise magnetization fields, respectively, and describe the electric and magnetic fluctuations within the material. Here, $\varepsilon(\mathbf{r}, \omega)$ and $\mu(\mathbf{r}, \omega)$ are the electric permittivity and magnetic permeability of the background medium and $\hat{\mathbf{f}}_\lambda(\mathbf{r}, \omega)$ and $\hat{\mathbf{f}}^\dagger_\lambda(\mathbf{r}, \omega)$ obey the usual bosonic commutation relation

$$[\,\hat{\mathbf{f}}_\lambda(\mathbf{r}, \omega), \hat{\mathbf{f}}^\dagger_{\lambda'}(\mathbf{r}', \omega')] = \delta_{\lambda\lambda'}\boldsymbol{\delta}(\mathbf{r} - \mathbf{r}')\delta(\omega - \omega'). \tag{7}$$

To compute how the fluctuations in the material affect the 'central spin' one needs to find the macroscopic fields that the Langevin noise generates. To do this one can return to Maxwell's equations and, by using the new 'noise' fields as source terms, the electromagnetic fields generated by the fluctuations can be found. The resulting equations read

$$\boldsymbol{\nabla} \cdot \hat{\mathbf{B}}(\mathbf{r}, \omega) = 0, \tag{8}$$

$$\boldsymbol{\nabla} \times \hat{\mathbf{E}}(\mathbf{r}, \omega) - \mathrm{i}\omega\hat{\mathbf{B}}(\mathbf{r}, \omega) = \mathbf{0}, \tag{9}$$

$$\boldsymbol{\nabla} \cdot \hat{\mathbf{D}}(\mathbf{r}, \omega) = \hat{\rho}_N(\mathbf{r}, \omega), \tag{10}$$

$$\boldsymbol{\nabla} \times \hat{\mathbf{H}}(\mathbf{r}, \omega) + \mathrm{i}\omega\hat{\mathbf{D}}(\mathbf{r}, \omega) = \hat{\mathbf{J}}_N(\mathbf{r}, \omega), \tag{11}$$

with the noise charge density and noise current density defined by $\hat{\rho}_N(\mathbf{r}, \omega) = \boldsymbol{\nabla} \cdot \hat{\mathbf{P}}_N$ and $\hat{\mathbf{J}}_N(\mathbf{r}, \omega) = -\mathrm{i}\omega\hat{\mathbf{P}}_N(\mathbf{r}, \omega) + \boldsymbol{\nabla} \times \hat{\mathbf{M}}_N(\mathbf{r}, \omega)$, respectively. Resubstituting equations (5) and (6) into Maxwell's equations, one can show that the magnetic field operator, which describes longitudinal magnetic fluctuations within the medium, is given by [12, 13]

$$\hat{b}_z(\mathbf{r}, \omega, t) = \frac{\mathrm{e}^{\mathrm{i}\omega t}}{\mathrm{i}\omega}\sum_{\lambda=e,m}\int \mathrm{d}^3r'\,\hat{z} \cdot \boldsymbol{\nabla} \times \boldsymbol{G}_\lambda(\mathbf{r}, \mathbf{r}', \omega) \cdot \hat{\mathbf{f}}_\lambda(\mathbf{r}', \omega). \tag{12}$$

Here, the coefficients $\boldsymbol{G}_\lambda(\mathbf{r}, \mathbf{r}', \omega)$ are defined as

$$\boldsymbol{G}_e(\mathbf{r}, \mathbf{r}', \omega) = \mathrm{i}\frac{\omega^2}{c^2}\sqrt{\frac{\hbar}{\pi\varepsilon_0}\,\mathrm{Im}\,\varepsilon(\mathbf{r}', \omega)}\,\boldsymbol{G}(\mathbf{r}, \mathbf{r}', \omega), \tag{13}$$

$$\boldsymbol{G}_m(\mathbf{r}, \mathbf{r}', \omega) = -\mathrm{i}\frac{\omega}{c}\sqrt{\frac{\hbar}{\pi\varepsilon_0}\frac{\mathrm{Im}\,\mu(\mathbf{r}', \omega)}{|\mu(\mathbf{r}', \omega)|^2}}\,[\boldsymbol{G}(\mathbf{r}, \mathbf{r}', \omega) \times \overleftarrow{\boldsymbol{\nabla}}'], \tag{14}$$

with the backward arrow referring to the fact that the operator acts on the right-hand variable (here r'). The function, $\boldsymbol{G}(\mathbf{r}, \mathbf{r}', \omega)$, is the electromagnetic Green's function, which is the solution to the Helmholtz equation for a point source

$$\boldsymbol{\nabla} \times \frac{1}{\mu(\mathbf{r}, \omega)}\boldsymbol{\nabla} \times \boldsymbol{G}(\mathbf{r}, \mathbf{r}', \omega) - \frac{\omega^2}{c^2}\varepsilon(\mathbf{r}, \omega)\boldsymbol{G}(\mathbf{r}, \mathbf{r}', \omega) = \delta(\mathbf{r} - \mathbf{r}'). \tag{15}$$

2.3. Spin decoherence

Substituting the operator for the magnetic fluctuations in equation (12) into the Hamiltonian in equation (3) and using it to evaluate the expression for the spin coherence in equation (4) leads to [14] (see supplementary information, which is available online at stacks.iop.org/NJP/22/033017/mmedia)

$$\phi(t) = \hbar\mu_0\gamma^2 t^2 \int_0^\infty \frac{\mathrm{d}\omega}{2\pi}\,\mathrm{sinc}^2(\omega t/2)\coth(\hbar\omega/2k_bT)\hat{z} \cdot \boldsymbol{\nabla} \times \mathrm{Im}\,\boldsymbol{G}(\mathbf{r}_s, \mathbf{r}_s, \omega) \times \overleftarrow{\boldsymbol{\nabla}} \cdot \hat{z}. \tag{16}$$

Here, the 'sinc' function is the usual free-induction decay noise filter function and the 'coth' function is the thermal boson occupation number. The imaginary part of the double curl of the Green's function gives the local density of states and, hence, the decoherence rate is proportional to the density of magnetic fluctuations at $\mathbf{r}_s$, the location of the 'central spin'.

For systems whose coherence evolves exponentially as $L = e^{-\Gamma\ t}$, the coherence time is easily defined as $T_2 = 1/\Gamma$ i.e. the time when the coherence has dropped to $L = e^{-1} = 36.8\%$. From equation (16) it is easy to see that the coherence dynamics of a 'central spin' is a complicated function of time, t and, hence it is not possibly to simply define the coherence time in terms of a simple exponential decay parameter. However, in the long time limit the 'sinc' function becomes nascent δ-function

$$\lim_{t\to\infty}\frac{t\ \mathrm{sinc}(\omega t/2)}{\pi} = \delta(\omega/2). \tag{17}$$

Thus, in the long time limit the coherence reduces to a simple exponential decay with the decay rate, Γ, given by

$$\Gamma = \hbar\mu_0\gamma^2 \lim_{\omega\to 0}[\coth(\hbar\omega/2k_bT)\hat{z} \cdot \boldsymbol{\nabla} \times \mathrm{Im}\,\boldsymbol{G}(\mathbf{r}_s, \mathbf{r}_s, \omega) \times \overleftarrow{\boldsymbol{\nabla}} \cdot \hat{z}]. \tag{18}$$

However, as $\coth(\alpha\omega) \sim 1/\alpha\omega$ as $\omega \to 0$, this limit only converges if the imaginary part of the double curl of the Green's function scales as $\hat{z} \cdot \boldsymbol{\nabla} \times \mathrm{Im}\,\boldsymbol{G}(\mathbf{r}_s, \mathbf{r}_s, \omega) \times \overleftarrow{\boldsymbol{\nabla}} \cdot \hat{z} \sim \omega^s$ with $s \geqslant 1$ as $\omega \to 0$. Although this result can give an reasonable estimate of the coherence time in some cases, it neglects the short time dynamics and hence will be a poor approximation in situations where the behavior of the 'central spin' around the initial time is important. In light of this, the results presented here will not use this approximation and for practical purposes the coherence time will be taken to be the time in which the coherence drops to $L = e^{-1} = 36.8\%$.

2.4. Regularization via local-field corrections

There is one last issue that needs to be addressed, namely that the double curl of the Green's function for a homogeneous medium in the coincident limit diverges if the absorption in the medium is non-zero. As previously mentioned, vanishing absorption over the full frequency range is forbidden by the Kramers–Krönig relations which, themselves, are a result of causality [16]. Hence, to properly model the coherence properties of a 'central spin' embedded in a realistic medium, a further step is required.

The divergences of the Green's function can be regularized by performing local-field corrections on the electromagnetic field at the location of the 'central spin' [14]. To perform these corrections one assumes that the spin is located at the center of a spherical cavity whose radius, R_c, is much smaller than the characteristic wavelength of the system [19, 20]. This procedure is the quantum mechanical equivalent of the Onsager model [21, 22], which is often used in physical chemistry to compute the effects of a dielectric medium on a polarizable molecule [23, 24]. The cavity is considered to be vacuum and hence free of noise sources and the interface with the surrounding material to be a simple 'step function' interface devoid of gradients, roughness or impurities. It is important to stress that the cavity used in this procedure is merely mathematical technique for computing the field corrections and does not represent anything physical. Essentially, the presence of a cavity introduces an 'ultraviolet' cutoff on the wavevector at $k \approx 2\pi/R_c$ and, hence, regularizes the Green's function.

With this construction, the Green's function can be split up into three parts [25, 26]

$$\boldsymbol{G}(\mathbf{r}, \mathbf{r}', \omega) = \boldsymbol{G}^{(1)}(\mathbf{r}, \mathbf{r}', \omega) + \boldsymbol{G}^{(2)}(\mathbf{r}, \mathbf{r}', \omega) + \boldsymbol{G}^{(3)}(\mathbf{r}, \mathbf{r}', \omega). \tag{19}$$

The first term is proportional to the reflective part of the cavity Green's function and gives the bulk decoherence rate that was studied in [14]. The second term is proportional to the transmissive part of the cavity Green's

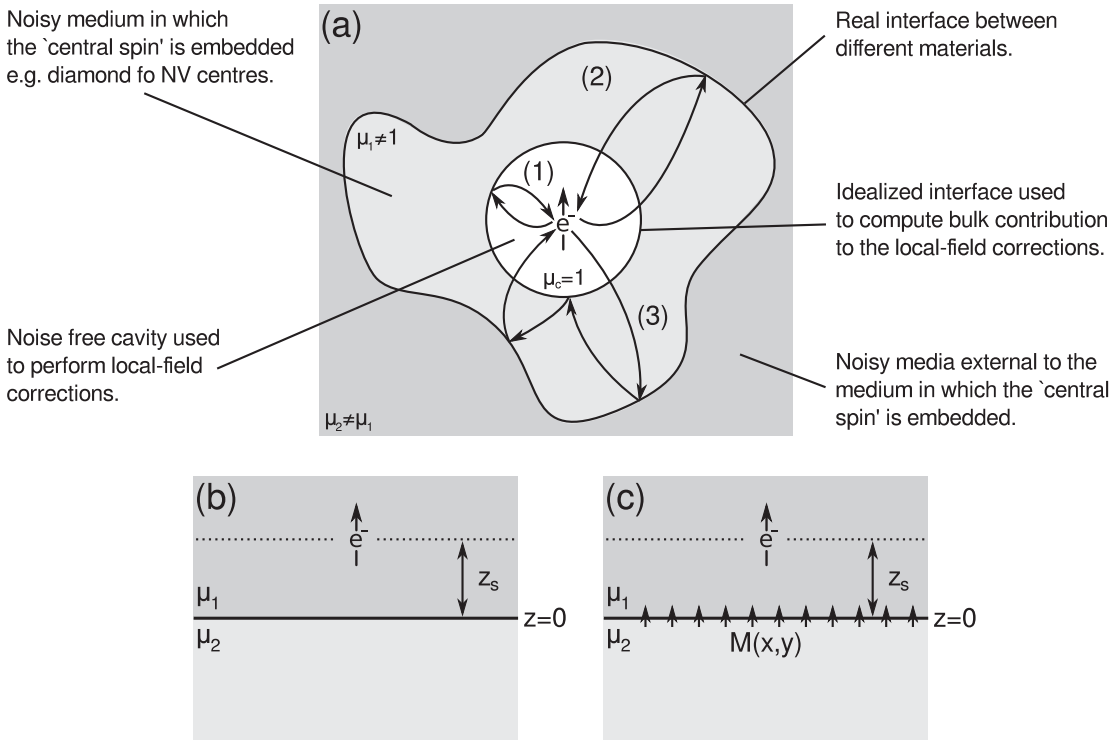

Figure 1. The interaction of a 'central spin' with an inhomogeneous background medium (a) schematic of the Green's function for a local-field corrected 'central spin' for general inhomogeneous media: (1) gives the bulk contribution and is proportional to the reflective part of the cavity Green's function, (2) gives the scattering part and is proportional to the transmissive part of the cavity Green's function and (3) gives the contribution from multiple scattering between the external side of the cavity and other homogeneities. This last term (3) is negligible. (b) and (c) Schematics of the interaction of a 'central spin' with a planar interface, a planar interface with a layer of surface spins (which results in a surface magnetization, $M(x, y)$), respectively, which are the specific examples of inhomogeneous media considered here.

function and gives the decoherence rate owing to the scattering from inhomogeneities external to the cavity. The final term gives the contribution from multiple scatting between the external side of the cavity and other inhomogeneities. As this last contribution scales as $\approx\omega R_c/c$ and the cavity radius, R_c, is assumed to be much smaller than the characteristic wavelength of the interaction, this term is negligible compared to the bulk and scattering contributions and, hence, will be neglected in the following. These contributions are shown schematically in figure 1(a).

2.5. The Green's function

Consider a 'central spin' located at the center ($\mathbf{r} = 0$) of a spherical cavity embedded in an inhomogeneous medium. The Green's function for the whole medium, including the spherical cavity, reads

$$\boldsymbol{G}^{(i)}(\mathbf{r}, \mathbf{r}', \omega) = \frac{\mathrm{i}k}{4\pi}\sum_{n\in e,o}\sum_{l=1}^{\infty}\sum_{m=0}^{l}(2-\delta_{l0})\frac{2l+1}{l(l+1)}\frac{(l-m)!}{(l+m)!} \times [\tilde{R}_{TE}(\omega)\boldsymbol{M}_{\mathrm{mln}}(k, \mathbf{r}) \otimes \boldsymbol{M}_{\mathrm{mln}}(k, \mathbf{r}') + \tilde{R}_{TM}(\omega)\boldsymbol{N}_{\mathrm{mln}}(k, \mathbf{r}) \otimes \boldsymbol{N}_{\mathrm{mln}}(k, \mathbf{r}')], \tag{20}$$

where $\tilde{R}_{TE}$ and $\tilde{R}_{TM}$ are the generalized reflection coefficients for the *TE* and *TM* polarized waves respectively and the $\boldsymbol{M}_{\mathrm{mln}}(k, \mathbf{r})$ and $\boldsymbol{N}_{\mathrm{mln}}(k, \mathbf{r})$ dyads are given by

$$\boldsymbol{M}_{ml\binom{e}{o}}(k, \mathbf{r}) = \mp\frac{m}{\sin\theta}j_l(kr)P_l^m(\cos\theta)\begin{pmatrix}\sin m\phi\\ \cos m\phi\end{pmatrix}\underline{e}_\theta - j_l(kr)\frac{\mathrm{d}P_l^m(\cos\theta)}{\mathrm{d}\theta}\begin{pmatrix}\cos m\phi\\ \sin m\phi\end{pmatrix}\underline{e}_\phi, \tag{21}$$

$$\boldsymbol{N}_{ml\binom{e}{o}}(k, \mathbf{r}) = \frac{l(l+1)}{kr}j_l(kr)P_l^m(\cos\theta)\begin{pmatrix}\cos m\phi\\ \sin m\phi\end{pmatrix}\underline{e}_r + \frac{1}{kr}\frac{\mathrm{d}}{\mathrm{d}r}[rj_l(kr)]\left[\frac{\mathrm{d}P_l^m(\cos\theta)}{\mathrm{d}\theta}\begin{pmatrix}\cos m\phi\\ \sin m\phi\end{pmatrix}\underline{e}_\theta \mp \frac{m}{\sin\theta}P_l^m(\cos\theta)\begin{pmatrix}\sin m\phi\\ \cos m\phi\end{pmatrix}\underline{e}_\phi\right], \tag{22}$$

where $j_l(x)$ are spherical Bessel functions of the first kind and $P_l^m(x)$ are the associated Legendre polynomials. Taking $\mathbf{r}, \mathbf{r}' \to 0$ one finds that the only contribution is from $l = 1$ and $m = 0$. Hence, the *TM* mode vanishes and the only contribution is from the *TE* mode. Thus, the Green's function reduces to

$$\hat{z}\cdot\boldsymbol{\nabla}\times\boldsymbol{G}(\mathbf{r},\mathbf{r}',\omega)\times\overleftarrow{\boldsymbol{\nabla}}\cdot\hat{z}|_{\mathbf{r},\mathbf{r}'\to 0}=\frac{3\mathrm{i}k}{8\pi}\tilde{R}_{TE}(\omega)\sum_{n\in e,o}\boldsymbol{\nabla}\times\boldsymbol{M}_{01n}(k,\mathbf{r})\otimes\boldsymbol{M}_{01n}(k,\mathbf{r}')\times\overleftarrow{\boldsymbol{\nabla}}|_{\mathbf{r},\mathbf{r}'\to 0}=\mathrm{i}\frac{\omega^3}{6\pi c^3}\tilde{R}_{TE}(\omega). \tag{23}$$

2.6. The bulk contribution

The bulk contribution is given by $\boldsymbol{G}^{(1)}(\mathbf{r},\mathbf{r}',\omega)$ which describes reflection from the walls of the spherical cavity (see figure 1(a)). In this case the generalized reflection coefficient is just the reflection coefficient for the spherical cavity $\tilde{R}_{TE}(\omega)=R_{TE}(\omega)$ which is given by the Mie scattering coefficient

$$R_{TE}(\omega)=\frac{h_1^{(1)}(z_0)[zh_1^{(1)}(z)]'-\mu(\omega)h_1^{(1)}(z)[z_0h_1^{(1)}(z_0)]'}{\mu(\omega)h_1^{(1)}(z)[z_0j_1^{(1)}(z_0)]'-j_1^{(1)}(z_0)[zh_1^{(1)}(z)]'}, \tag{24}$$

where $z_0=\omega R_c/c$ and $z=n(\omega)\omega R_c/c$, with R_c the radius of the cavity, and $j_1(z)$ and $h_1(z)$, respectively, the spherical Bessel and Hankel functions of the first kind for $l=1$

$$j_1(z)=\frac{\sin(z)}{z^2}-\frac{\cos(z)}{z}, \tag{25}$$

$$h_1(z)=\left(\frac{1}{z}+\frac{\mathrm{i}}{z^2}\right)\mathrm{e}^{\mathrm{i}z}. \tag{26}$$

Following [14], we will assume that R_c is small compared to the main wavelengths associated with the decoherence process (in fact the free induction decay filter is the square of the 'sinc' function and, hence, is strongly peaked around $\omega=0$ so the main wavelength $\to\infty$) and we expand $R_{TE}(\omega)$ in powers of $\omega R_c/c$

$$R_{TE}(\omega)=\frac{3\mu(\omega)-3}{[2\mu(\omega)+1]}\frac{\mathrm{i}c^3}{\omega^3R_c^3}+\frac{9}{5}\left\{\frac{\mu(\omega)^2[5\varepsilon(\omega)-1]-3\mu(\omega)-1]}{[2\mu(\omega)+1]^2}\right\}\frac{\mathrm{i}c}{\omega R_c}-9\frac{\mu(\omega)^{5/2}\varepsilon(\omega)^{3/2}}{[2\mu(\omega)+1]^2}+1+\mathcal{O}\left(\frac{\omega R_c}{c}\right). \tag{27}$$

By taking the reflection coefficient to leading order and substituting the result into equation (23), one finds

$$\hat{z}\cdot\boldsymbol{\nabla}\times\boldsymbol{G}^{(1)}(\mathbf{r}_s,\mathbf{r}_s,\omega)\times\overleftarrow{\boldsymbol{\nabla}}\cdot\hat{z}=\frac{1}{2\pi R_c^3}\frac{1-\mu(\omega)}{1+2\mu(\omega)}. \tag{28}$$

Substituting the result into equation (16) leads to

$$\phi(t)=\frac{\hbar\mu_0\gamma^2t^2}{2\pi R_c^3}\int_0^\infty\frac{\mathrm{d}\omega}{2\pi}\,\mathrm{sinc}^2(\omega t/2)\coth(\hbar\omega/2k_bT)\,\mathrm{Im}\left[\frac{1-\mu(\omega)}{1+2\mu(\omega)}\right]. \tag{29}$$

2.7. The scattering contribution

In inhomogeneous media, one obtains a further contribution to the decoherence rate which is cause by scattering off surfaces external to the spherical cavity (see figure 1(a)). This contribution is given by $\boldsymbol{G}^{(2)}(\mathbf{r},\mathbf{r}',\omega)$ which describes waves that are transmitted through the surface of the spherical cavity, scatter off an external inhomogeneity and are then transmitted back into the cavity. In this case the generalized reflection coefficient is given by $\tilde{R}_{TE}=T_{TE}^{\mathrm{out}}\tilde{R}_{TE}^{\mathrm{ext}}T_{TE}^{\mathrm{in}}$ where T_{TE}^{out} is the transmission coefficient for outgoing waves through the wall of the spherical cavity, T_{TE}^{in} is the transmission coefficient for incoming waves through the wall of the spherical cavity and $\tilde{R}_{TE}^{\mathrm{ext}}$ is the generalized reflection coefficient for all other interfaces external to the cavity. The appropriate Mie scattering coefficients read

$$T_{TE}^{\mathrm{out}}(\omega)=\frac{-\mathrm{i}\mu(\omega)}{z_0(j_1^{(1)}(z_0)[zh_1^{(1)}(z)]'-\mu(\omega)h_1^{(1)}(z)[z_0h_1^{(1)}(z_0)]')}, \tag{30}$$

and

$$T_{TE}^{\mathrm{in}}(\omega)=\frac{-\mathrm{i}}{z(j_1^{(1)}(z_0)[zh_1^{(1)}(z)]'-\mu(\omega)h_1^{(1)}(z)[z_0h_1^{(1)}(z_0)]')}. \tag{31}$$

As before we expand these coefficients for small values of $\omega R_c/c$ to give

$$T_{TE}^{\mathrm{out}}(\omega)=\frac{3}{1+2\mu(\omega)}\mu(\omega)n(\omega)^2+\mathcal{O}\left(\frac{\omega R_c}{c}\right), \tag{32}$$

and

$$T_{TE}^{\text{in}}(\omega) = \frac{3}{1 + 2\mu(\omega)} n(\omega) + \mathcal{O}\left(\frac{\omega R_c}{c}\right), \tag{33}$$

where $n(\omega) = \sqrt{\varepsilon(\omega)\mu(\omega)}$ is the refractive index. Thus, this part of the Green's function to zeroth order in $\omega R_c/c$ becomes

$$\hat{z} \cdot \boldsymbol{\nabla} \times \boldsymbol{G}^{(2)}(\mathbf{r}, \mathbf{r}', \omega) \times \overleftarrow{\boldsymbol{\nabla}} \cdot \hat{z}|_{\mathbf{r},\mathbf{r}'\to 0} = \left(\frac{3}{1 + 2\mu(\omega)}\right)^2 \left[\mathrm{i}\mu(\omega)\frac{\omega^3 n(\omega)^3}{6\pi c^3}\tilde{R}_{\mathrm{i}}^{\text{ext}}\right]. \tag{34}$$

The term in square brackets is just the scattering Green's function in the coincident limit for a medium without the spherical cavity, hence we can write

$$\hat{z} \cdot \boldsymbol{\nabla} \times \boldsymbol{G}^{(2)}(\mathbf{r}, \mathbf{r}', \omega) \times \overleftarrow{\boldsymbol{\nabla}} \cdot \hat{z}|_{\mathbf{r},\mathbf{r}'\to 0} = \left(\frac{3}{1 + 2\mu(\omega)}\right)^2 \hat{z} \cdot \boldsymbol{\nabla} \times \boldsymbol{G}^{(S)}(\mathbf{r}_s, \mathbf{r}_s, \omega) \times \overleftarrow{\boldsymbol{\nabla}} \cdot \hat{z}, \tag{35}$$

where $G^{(S)}(\mathbf{r}, \mathbf{r}', \omega)$ is the scattering Green's function for the medium without the spherical cavity. Thus, the decoherence owing to inhomogeneities in the background medium is given by

$$\phi(t) = 9\hbar\mu_0\gamma^2 t^2 \int_0^\infty \frac{\mathrm{d}\omega}{2\pi} \operatorname{sinc}^2(\omega t/2) \coth(\hbar\omega/2k_b T) \operatorname{Im}\left[\frac{1}{[1 + 2\mu(\omega)]^2} \hat{z} \cdot \boldsymbol{\nabla} \times \boldsymbol{G}^{(S)}(\mathbf{r}_s, \mathbf{r}_s, \omega) \times \overleftarrow{\boldsymbol{\nabla}} \cdot \hat{z}\right]. \tag{36}$$

The expression in equation (36) is valid for any geometry—one just needs to substitute in the appropriate Green's function. As an example, we will now compute the coherence time of a 'central spin' for a specific inhomogeneous medium, namely a planar half-space.

3. Decoherence close to a surface

3.1. Decoherence from the interface

A 'central spin' inside a medium close to a surface can be modeled by considering a planar half-space with a single interface at $z = 0$. Here, the upper half plane, labeled 1, consists of a medium within which the spin is located and the lower half plane, labeled 2, corresponding to an external environment (see figure 1(b)). Taking the coincident limit of the double curl of the single half-space Green's function [13, 27], converting to polar coordinates and computing the angular part of the integral leads to (see supplementary information)

$$\hat{z} \cdot \boldsymbol{\nabla} \times \boldsymbol{G}(\mathbf{r}_s, \mathbf{r}_s, \omega) \times \overleftarrow{\boldsymbol{\nabla}} \cdot \hat{z} = \frac{\mathrm{i}\mu_1(\omega)}{4\pi} \int_0^\infty \mathrm{d}k_p \, \frac{k_p^3}{k_{z,1}} \mathrm{e}^{2\mathrm{i}k_{z,1}|z_s|} R_{TE}, \tag{37}$$

with $k_{z,i} = \sqrt{k_i^2 - k_p^2}$, $k_i = n_i(\omega)\omega/c$ and the reflection coefficient for the TE mode given by

$$R_{TE} = \frac{\mu_2(\omega)k_{z,1} - \mu_1(\omega)k_{z,2}}{\mu_2(\omega)k_{z,1} + \mu_1(\omega)k_{z,2}}. \tag{38}$$

Once again we see that only the *TE* component of the wave contributes. Owing to the highly oscillatory nature of the Greens' function as a function of frequency, computing both the integral over k_p in equation (37) and ω in equation (36) numerically is computationally highly intensive. Furthermore, as the 'sinc' function diverges at $\omega \to +\infty$ it is not possible to convert the frequency integral to the usual Matsubara summation. However, the free induction decay filter is strongly peaked about $\omega = 0$ ($\lambda \to \infty$) and the distance from the 'central spin' to the surface is typically on the order of tens of nanometers. This means that the 'central spin' is within a wavelength of the surface and, hence, one can use a near field expansion to obtain an analytical approximation for the Green's function. In this limit $z_s \ll \lambda = 2\pi n(\omega)/k$. Thus, $k \ll k_p$ and we can expand k_z as

$$k_z = \sqrt{k^2 - k_p^2} = \mathrm{i}k_p\sqrt{1 - \frac{k^2}{k_p^2}} \approx \mathrm{i}k_p. \tag{39}$$

Hence, the reflection coefficient simplifies to

$$R_{TE} \approx \frac{\mu_2(\omega) - \mu_1(\omega)}{\mu_2(\omega) + \mu_1(\omega)}, \tag{40}$$

and the integral to

$$\hat{z} \cdot \boldsymbol{\nabla} \times \boldsymbol{G}(\mathbf{r}_s, \mathbf{r}_s, \omega) \times \overleftarrow{\boldsymbol{\nabla}} \cdot \hat{z} = \frac{\mu_1(\omega)}{4\pi} \frac{\mu_2(\omega) - \mu_1(\omega)}{\mu_2(\omega) + \mu_1(\omega)} \int_0^\infty \mathrm{d}k_p \, k_p^2 \mathrm{e}^{-2k_p|z_s|}, \tag{41}$$

which can be integrated analytically to give

$$\hat{z}\cdot\boldsymbol{\nabla}\times\boldsymbol{G}(\mathbf{r}_s,\mathbf{r}_s,\omega)\times\overleftarrow{\boldsymbol{\nabla}}\cdot\hat{z}=\frac{\mu_1(\omega)}{16\pi|z_s|^3}\frac{\mu_2(\omega)-\mu_1(\omega)}{\mu_2(\omega)+\mu_1(\omega)}. \tag{42}$$

Essentially, the Green's function comprises of two contributions, a propagating contribution and an evanescent (decaying) contribution. The near-field expansion neglects the propagating contribution in favor of the dominant evanescent contribution.

Substituting equation (42) into (36) one finds that the surface contribution to the spin coherence reads

$$\phi(t)=\frac{9\hbar\mu_0\gamma^2t^2}{16\pi|z_s|^3}\int_0^\infty\frac{\mathrm{d}\omega}{2\pi}\,\mathrm{sinc}^2(\omega t/2)\coth(\hbar\omega/2k_bT)\,\mathrm{Im}\left[\frac{\mu_1(\omega)}{[1+2\mu_1(\omega)]^2}\frac{\mu_2(\omega)-\mu_1(\omega)}{\mu_2(\omega)+\mu_1(\omega)}\right]. \tag{43}$$

The result exhibits the same z_s^{-3} scaling that was found in previous phenomenological models [11]. However, here we find the decoherence rate is also a function of the frequency dependent permeabilities μ_1 and μ_2 of the upper and lower layers. Hence, not only are the magnetic properties of the layer in which the spin is embedded important when determining the coherence time of the spin but the magnetic properties of the neighboring layer also play a role.

3.2. Decoherence from surface spins

Another effect that has been discussed [10] is the effect of spins that lie on the surface of the medium in which the 'central spin' is embedded. One can model the effect of spins located on the surface of the medium by assuming that they induce a surface magnetization (see figure 1(c)). This surface magnetization can then, in turn, be modeled as being generated by an 'effective' bound current. Here, we assume that the surface spins are, primarily, a source of static magnetization rather than an additional noise source but are able respond to perturbations in the magnetic field owing to noise fluctuations in the bulk. The traditional expression of a bound current is, $\mathbf{K}_m=\mathbf{M}\times\hat{n}$, where $\hat{n}$ is the unit vector normal to the surface. This implies that both the current and the magnetization is in the plane of the surface. However, surface spins are not inhibited by such restrictions and can orientate themselves at any angle to the surface. This means that the 'effective' current need not orientated in the plane of the surface. The fluctuating fields that cause decoherence are those that are orientated parallel to the spin, which in this case is the z-direction. Hence, we write our 'effective' spin magnetization current as $\mathbf{K}_s=\mathbf{M}\times\hat{x}$. This 'effective' spin magnetization current leads to an extra term in the electromagnetic jump conditions at the interface and, hence, an extra term in the reflection coefficients for the surface.

The spins on the surface of the material can respond to an applied magnetic field. In the linear response regime, one can related the magnetization of the surface spins to the applied magnetic field via $\mathbf{M}=\chi_s(\omega)\mathbf{H}_s$, where $\chi_s(\omega)$ is the 2D surface susceptibility of the surface spins and $\mathbf{H}_s$ is the magnetic field at the surface. However, $\mathbf{H}_s$ is, *a priori*, unknown. As an approximation, we can use the magnetic field at the interface in the absence of surface spins make an estimate of $\mathbf{H}_s$. In analogy with quantum mechanics, this would be equivalent to a first order Born approximation with the magnetic field without the surface spins equivalent to the unperturbed 'free' field state and surface spins acting as the scattering potential. This approximation is valid when the scattering is small. Here, we assume that the density of the spins on the surface of the medium is smaller than those in the bulk and, hence, the susceptibility, $\chi_s(\omega)\ll\chi_1(\omega)$, $\chi 2(\omega)$ and, therefore, the 'scattering' of the magnetic field owing to the surface spins is small.

The presence of this extra magnetization field the reflection coefficient at the surface becomes (see supplementary information)

$$R_{TE}=\frac{k_{1,z}\mu_2(\omega)-k_{2,z}\mu_1(\omega)}{k_{1,z}\mu_2(\omega)+k_{2,z}\mu_1(\omega)}-\frac{2\mathrm{i}k_p^2k_{1,z}\chi_s(\omega)\mu_1(\omega)\mu_2(\omega)}{[k_{1,z}\mu_2(\omega)+k_{2,z}\mu_1(\omega)]^2}. \tag{44}$$

The first term in equation (44) is the usual reflection coefficient for a surface without surface spins and the second term gives the reflection owing to the magnetization field of the surface spins. In this case the Green's function has the same form as before (equation (37)) except with the reflection coefficient of the surface (including the surface spin layer) now given by the (44). Applying the same near field approximation and analytically integrating the result leads to

$$\hat{z}\cdot\boldsymbol{\nabla}\times\boldsymbol{G}(\mathbf{r}_s,\mathbf{r}_s,\omega)\times\overleftarrow{\boldsymbol{\nabla}}\cdot\hat{z}=\frac{\mu_1}{16\pi|z_s|^3}\frac{\mu_2(\omega)-\mu_1(\omega)}{\mu_2(\omega)+\mu_1(\omega)}-\frac{3\mu_1(\omega)}{16\pi|z_s|^4}\frac{\chi_s(\omega)\mu_1(\omega)\mu_2(\omega)}{[\mu_1(\omega)+\mu_2(\omega)]^2}. \tag{45}$$

The first term is the same as for the case of a single interface with no surface spins. The second term gives the contribution from the surface spins alone. Thus, the surface spin contribution to the spin coherence reads

$$\phi(t) = -\frac{27\hbar\mu_0\gamma^2 t^2}{16\pi|z_s|^4}\int_0^\infty \frac{\mathrm{d}\omega}{2\pi}\,\mathrm{sinc}^2(\omega t/2)\coth(\hbar\omega/2k_bT)\,\mathrm{Im}\left[\frac{\mu_1(\omega)}{[1+2\mu_1(\omega)]^2}\frac{\chi_s(\omega)\mu_1(\omega)\mu_2(\omega)}{[\mu_1(\omega)+\mu_2(\omega)]^2}\right]. \quad (46)$$

Again, we see that the expression displays both the z_s^{-4} scaling and the linear dependence in the surface spin susceptibility that has been found in previous phenomenological models [10]. Note that, in this case the imaginary term is, in general, negative so the coherence still exponentially decays.

4. Results

4.1. Permeability models

In order to validate the theoretical results we will compute the depth dependence of the decoherence of a shallow *NV* center in diamond, which was measured experientially in [8, 9].

First, consider the case of a single interface without the presence of surface spins such as depicted in figure 1(b). Here, the material with permeability μ_1 in which the spin is located is diamond. The interface at $z = 0$ depicts an interface with another material with permeability, μ_2. For the experiments documented in [8, 9] this other medium is just the vacuum ($\mu_2 = 1$).

In this system the main source of decoherence comes from the ^{13}C nuclear spins, which are present at a concentration of ≈1.1% in the electronic-grade diamond used in the experiments. In this formalism, the effect of the nuclear spins is described by the magnetic permeability, μ_i. We can use the common frequency dependent paramagnetic permeability model [28]

$$\mu_i(\omega) = \frac{\chi_i}{1+\mathrm{i}\omega\tau} + 1, \quad (47)$$

to model the magnetic response in ith layer. Here, χ is the magnetic susceptibility of the nuclear spins and τ is the magnetization relaxation time (i.e. the time it takes the background spins to de-align when the magnetic field is switched off). In this model the static permeability ($\omega \to 0$) is give by $\chi_i + 1$ and at high frequencies ($\omega \to \infty$) $\mu(\omega) \to 1$ and, hence, the medium becomes transparent. The vacuum ($\mu(\omega) \to 1$) occurs when $\chi_i = 0$.

Although, we do not know the susceptibility of the ^{13}C nuclear spins in layer $i = 1$ precisely, we can make an order of magnitude estimate by noting that the susceptibility of unpaired electrons in paramagnetic atoms is on the order of $\chi \approx 1 \times 10^{-5}$. However, the coupling of electron spins to magnetic fields is much stronger than that of nuclear spins. The difference is quantified by the square of the gyromagnetic ratio. The gyromagnetic ratio for an electron is $\gamma = 1.76 \times 10^{11}$ rads s^{-1} T^{-1} whereas the gyromagnetic ratio for ^{13}C nuclear spins is over three orders of magnitude smaller, $\gamma_I = 6.73 \times 10^7$ rads s^{-1} T^{-1}. Scaling the paramagnetic susceptibility with regard to the weaker coupling and lower concentration of nuclear spins leads to an estimate the nuclear susceptibility on the order of $\chi_1 \approx 1.6 \times 10^{-14}$. The relaxation time is estimated to be $\tau_1 \approx 3$ ms from NMR linewidth measurements [29]. For the $i = 2$ layer we take χ_2 and τ_2 to be variables of a similar order of magnitude to represent materials with different magnetic responses.

In the second case, consider a single interface with the presence of surface spins such as depicted in figure 1(c). The material parameters of the diamond can be estimated in the same way as before. In addition, we can estimate the susceptibility of the surface spins in a similar way by assuming that they respond in the same manner as the nuclear spins and hence they obey the same frequency dependent model

$$\chi_s(\omega) = \frac{\chi_s^0}{1+\mathrm{i}\omega\tau_s}. \quad (48)$$

Reference [10] found the density of surface spins to be $\rho_{\mathrm{spins}} = 0.04$ nm^{-2}, which is about two orders of magnitude smaller than the density of the bulk ^{13}C nuclear spins, hence we take $\chi_s^0 \approx 10^{-16}$. Reference [10] also gives the surface spin relaxation rate to be $\tau_s = 5\ \mu$s.

Finally, when computing the bulk coherence time, a value of $R_c \approx 0.8$ nm was used, which is the average distance from the 'central spin' to the nearest nuclear spin and the temperature in all cases was taken to be 40 K.

4.2. Decoherence from the interface

Figure 2 shows the coherence time for an *NV* center as a function of distance for interfaces between diamond and various magnetically responding materials. In figures 2(a) and (b) $\tau_1 = \tau_2 = 3$ ms and χ_2 is varied. $\chi_2 = 0$ models the interface of diamond with the vacuum, where as $\chi_2 > 0$ models the interface of diamond materials with ever increasing magnetic responses. Figure 2(a) shows that for $\chi_2 \leqslant \chi_1$ the coherence time decreases as the *NV* center moves closer to the interface. Conversely, as the *NV* center moves away from the interface the coherence time approaches the homogeneous medium coherence time and, at distance greater of over 1 nm the effect of the interface is negligible. Furthermore, as the value of χ_2 approaches the value of χ_1 the coherence time increases. This is because, as the magnetic responses of the two materials becomes closer, the reflection

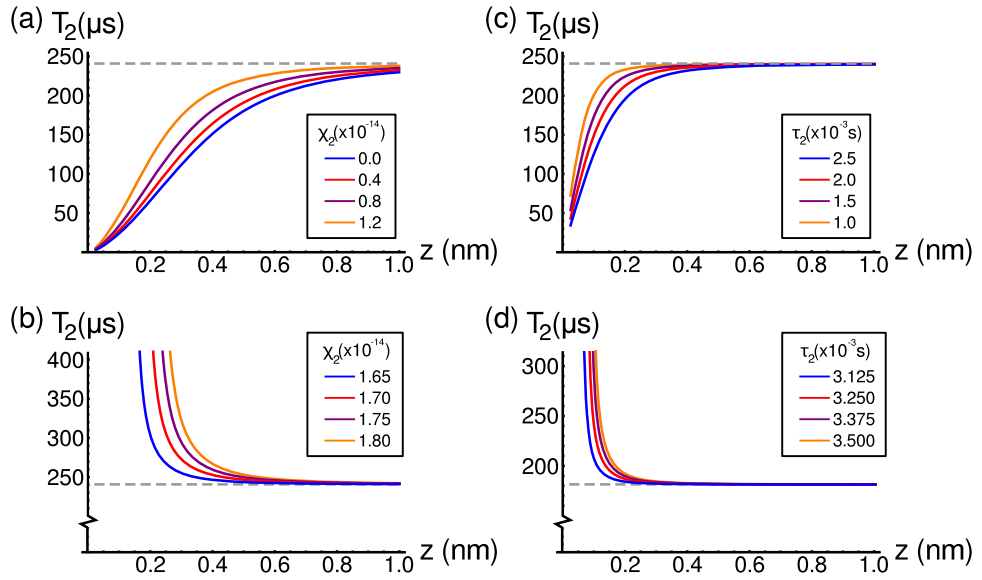

Figure 2. *NV* center decoherence close to an interface (a) and (b) decoherence of an *NV* center in diamond close to a interface for various magnetic susceptibilities, χ_2, of the adjoining material. (a) Show the case for $\chi_2 \leqslant \chi_1$ and (b) shows the case where $\chi_2 \geqslant \chi_1$. In both cases $\tau_2 \approx 3$ ms. The gray dashed line indicates the coherence time of an *NV* center in homogeneous bulk diamond with $\chi_1 = \chi_2 = 1.6 \times 10^{-14}$ and $\tau_1 = \tau_2 = 3$ ms. (c) and (d) Decoherence of an *NV* center in diamond close to a interface for various magnetic relaxation rates, τ_2, of the adjoining material. (c) Show the case for $\tau_2 \leqslant \tau_1$ and (d) shows the case where $\tau_2 \geqslant \tau_1$. In both cases $\chi_2 = 1.6 \times 10^{-14}$. Again, the gray dashed line indicates the coherence time of an *NV* center in homogeneous bulk diamond with $\chi_1 = \chi_2 = 1.6 \times 10^{-14}$ and $\tau_1 = \tau_2 = 3$ ms. In all cases $\chi_1 = 1.6 \times 10^{-14}$ and $\tau_1 = 3$ ms. The coherence time is taken to be the time taken for the coherence to drop to $L = e^{-1} = 36.8\%$.

coefficient at the interface is smaller and, hence, fewer magnetic fluctuations are reflected. Note that, if the two magnetic responses are equal then the material in the two layers is the same and there is no interface at all, and the coherence time is equal to the the homogeneous medium value.

Figure 2(b) shows that for $\chi_2 \geqslant \chi_1$ the coherence time increases as the *NV* center moves closer to the interface. This is because the phase shift that occurs on reflection from a strongly magnetically responding material leads to destructive interference of the magnetic fluctuations close to the interface. This effect might contribute to the suppression of decoherence at very short distances from the interface that was observed in [9]. Similarly, the larger χ_2 the longer the coherence time because the phase shift is greater and, hence, the incident and reflected magnetic fluctuations are further out of phase and, thus, the destructive interference is stronger.

In figures 2(c) and (d) $\chi_2 = 1.6 \times 10^{-14}$ in both layers and τ_2 is varied. Again, we see that the coherence time decreases as the *NV* center moves closer to the interface when $\tau_2 \leqslant \tau_1$ and increases for $\tau_2 \geqslant \tau_1$. This is, again, owing to the phase shift of the reflected fluctuations. For $\tau_2 \leqslant \tau_1$ the longer the relaxation time the shorter the coherence time. This is because the magnetic fluctuations persist for longer and, hence, have more of an effect on the *NV* center.

4.3. Decoherence from surface spins

Figures 3(a) and (b) show the coherence time for an *NV* center as a function of distance from an interface between diamond and the vacuum ($\chi_2 = 0$) in the presence of surface spins. In figure 3(a) $\tau_s = 5$ μs and χ_s is varied. The susceptibility of the surface spins is taken to be between 1% and 4% of the bulk nuclear spin susceptibility. As ever, the coherence time decreases as the *NV* center moves closer to the interface and the larger the surface spin susceptibility the shorter the coherence time. In figure 3(b) $\chi_s = 1.6 \times 10^{-16}$ m and τ_s is varied. Here, as before, the coherence time decreases as the *NV* center moves closer to the interface and the longer the relaxation time the shorter the coherence time. An important feature to note is that the distance over which the surface spins effect the *NV* center; the coherence time approaches the homogeneous medium coherence time at a depth of 50 nm, which is between 1 and 2 orders of magnitude larger than the distance range over which the interface alone interacts. Hence for shallow *NV* centers with depths greater than 1 nm the dominant decoherence method is the interaction with the surface spins. The interaction with the interface itself is negligible. These distances are the same order of magnitude as those found experimentally in [8, 9].

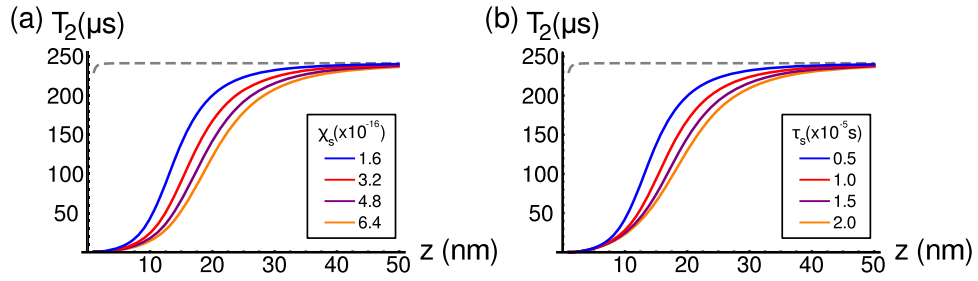

Figure 3. *NV* center decoherence in the presence of surface spins (a) decoherence of an *NV* center in diamond close to a interface with the vacuum for various area densities of surface spins and $\tau_s = 5\ \mu$s. The gray dashed line indicates the coherence time of an *NV* center close to an interface with the vacuum in the absence of surface spins. (b) Decoherence of an *NV* center in diamond close to a interface with the vacuum for various surface spin relaxation times and $\chi_s = 1.6 \times 10^{-16}$ m. The gray dashed line indicates the coherence time of an *NV* center close to an interface with the vacuum in the absence of surface spins. In all cases $\chi_1 = 1.6 \times 10^{-14}, \tau_1 = 3$ ms, $\chi_2 = 0$ and $\tau_2 = 0\ \mu$s. The coherence time is taken to be the time taken for the coherence to drop to $L = e^{-1} = 36.8\%$.

5. Summary

Here, we have extended the Green's function formalism for spin decoherence in a bulk material that was developed in [14] to inhomogeneous media. To validate the theory we have computed the decoherence rate of a shallow *NV* center in diamond placed within 50 nm from the surface. In the presence of surface spins, the coherence time decreases as one approaches the surface from a value of ≈240 μs at 50 nm to a value on the order of 10 μs for distances less than 10 nm. These coherence times are a similar order of magnitude to those found experimentally in [8, 9]. For a more precise estimate of the coherence times one would need more sophisticated permeability models and more accurate values for the magnetic properties of the ^{13}C spins in diamond and of any adjoining materials. However, these results show that the Green's function formalism is able to model decoherence in inhomogeneous spins systems. The formalism also shows that at distances greater than 1 nm it is the interaction with the surface spins that is dominant as opposed to the interaction with the interface itself. Experimental work in [9] showed that the influence of the interface falls off for distances >8 nm and hence the Green's function formalism also gives the correct order of magnitude result for this feature as well.

Acknowledgments

This work was supported by the National Science Foundation of China Research Grant No. 11750110420.

ORCID iDs

J A Crosse https://orcid.org/0000-0002-8378-4976

References

[1] Loss D and DiVincenzo D P 1998 Quantum computation with quantum dots *Phys. Rev.* A **57** 120
[2] Imamog¯lu A, Awschalom D D, Burkard G, DiVincenzo D P, Loss D, Sherwin M and Small A 1999 Quantum information processing using quantum dot spins and cavity QED *Phys. Rev. Lett.* **83** 4204
[3] Leggert A J, Chakravarty S, Dorsey T, Fisher M P A, Garg A and Zwerger W 1987 Dynamics of the dissipative two-state system *Rev. Mod. Phys.* **59** 1
[4] Yang W, Ma W-L and Liu R-B 2017 Quantum many-body theory for electron spin decoherence in nanoscale nuclear spin baths *Rep. Prog. Phys.* **80** 016001
[5] Tyryshkin A M, Morton J J, Benjamin S C, Ardavan A, Briggs G A D, Ager J W and Lyon S A 2006 Coherence of spin qubits in silicon *J. Phys.: Condens. Matter* **18** S783
[6] Dobrovitski V V, Fuchs G D, Falk A L, Santori C and Awschalom D D 2013 Quantum control over single spins in diamond *Annu. Rev. Condens. Matter Phys.* **4** 23
[7] Ma W-L, Wolfowicz G, Zhao N, Li S-S, Morton J J L and Liu R-B 2014 Uncovering many-body correlations in nanoscale nuclear spin baths by central spin decoherence *Nat. Commun.* **5** 4822
[8] Wang J *et al* 2016 Coherence times of precise depth controlled NV centers in diamond *Nanoscale* **8** 5780
[9] Zhang W *et al* 2017 Depth-dependent decoherence caused by surface and external spins for NV centers in diamond *Phys. Rev.* B **96** 235443
[10] Myers B A, Das A, Dartiailh C, Ohno K, Awschalom D D and Bleszynski Jayich A C 2014 Probing surface noise with depth-calibrated spins in diamond *Phys. Rev. Lett.* **113** 027602
[11] Pham L M *et al* 2016 NMR technique for determining the depth of shallow nitrogen-vacancy centers in diamond *Phys. Rev.* B **93** 045425
[12] Scheel S and Buhmann S Y 2008 Macroscopic quantum electrodynamics—concepts and applications *Acta Phys. Slovaca* **58** 675
[13] Buhmann S Y 2012 *Dispersion Forces I* (Berlin: Springer)

[14] Crosse J A 2019 Local-field corrections as a regularization method for the spin-boson model *Sci. Rep.* **9** 5216
[15] Reid M T H and Johnson S G 2015 Efficient computation of power, force, and torque in BEM scattering calculations *IEEE Trans. Antennas Propag.* **63** 3588
[16] Jackson J D 1999 *Classical Electrodynamics* (New York: Wiley)
[17] Huttner B and Barnett S M 1992 Quantization of the electromagnetic field in dielectrics *Phys. Rev.* A **46** 4306
[18] Suttorp L G and Wubs M 2004 Field quantization in inhomogeneous absorptive dielectrics *Phys. Rev.* A **70** 013816
[19] Glauber R J and Lewenstein M 1991 Quantum optics of dielectric media *Phys. Rev.* A **43** 467
[20] Scheel S, Knöll L and Welsch D-G 1999 Spontaneous decay of an excited atom in an absorbing dielectric *Phys. Rev.* A **60** 4094
[21] Onsager L 1936 Electric moments of molecules in liquids *J. Am. Chem. Soc.* **58** 1486
[22] Hill N E, Vaughn W E, Price A H and Davis M 1969 *Dielectric Properties and Molecular Behaviour* (New York: Van Nostrand Reinhold Company)
[23] Gilmore J and McKenzie R H 2005 Spin boson models for quantum decoherence of electronic excitations of biomolecules and quantum dots in a solvent *J. Phys.: Condens. Matter* **17** 1735
[24] Kirchberg H, Nalbach P and Thorwart M 2018 Nonequilibrium quantum solvation with a time-dependent Onsager cavity *J. Chem. Phys.* **148** 164301
[25] Dung H T, Buhmann S Y and Welsch D-G 2006 Local-field correction to the spontaneous decay rate of atoms embedded in bodies of finite size *Phys. Rev.* A **74** 023803
[26] Sambale A, Buhmann S Y, Welsch D-G and Tomaš M-S 2007 Local-field correction to one- and two-atom van der Waals interactions *Phys. Rev.* A **75** 042109
[27] Chew W C 1995 *Waves and Fields in Inhomogeneous Media* (Piscataway, NJ: IEEE)
[28] Sláma J, Krivošík P and Jančárik V 2000 Modification of permeability components modelling *J. Magn. Magn. Mater.* **215** 641
[29] Zhou J *et al* 1994 Study of natural diamonds by dynamic nuclear polarization-enhanced ^{13}C nuclear magnetic resonance spectroscopy *Solid State Nucl. Magn. Reson.* **3** 339